Kobe University Repository : Kernel

PDF issue: 2026-11-05

Hepatitis C virus NS3 protein interacts with ELKS-δ and ELKS-α, members of a novel protein family involved in intracellular transport and secretory pathways

Hidajat, Rachmat ; Nagano-Fujii, Motoko ; Deng, Lin ; Tanaka, Motofumi ; Takigawa, Yuki ; Kitazawa, Sohei ; Hotta, Hak

(Citation)
Journal of General Virology,86(8):2197-2208

(Issue Date)
2005-08

(Resource Type)
journal article

(Version)
Accepted Manuscript

(URL)
https://hdl.handle.net/20.500.14094/90000059

Hepatitis C virus NS3 protein interacts with ELKS-δ and ELKS-α, members of a novel protein family involved in intracellular transport and secretory pathways

Running title : HCV NS3 interacts with ELKS-δ and ELKS-α

Rachmat Hidajat,[1] Motoko Nagano-Fujii,[1] Lin Deng,[1] Motofumi Tanaka,[1,2] Yuki Takigawa,[1] Sohei Kitazawa,[3] and Hak Hotta[1,*]

Divisions of Microbiology,[1] Gastroenterological Surgery,[2] and Molecular Pathology,[3]

Kobe University Graduate School of Medicine, Kobe 650-0017, Japan.

The word count for the abstract: 242

The word count (text + figure legends): 5,484 (4,399 + 1,085)

Number of figures: 7 figures

*Correspondence: Mailing address: Division of Microbiology, Kobe University Graduate School of Medicine, 7-5-1 Kusunoki-cho, Chuo-ku, Kobe 650-0017, Japan.

Phone: +81-78-382-5500. Fax: +81-78-382-5519. E-mail: hotta@kobe-u.ac.jp

Supplementary material is available in JGV Online.

ABSTRACT

The NS3 protein of hepatitis C virus (HCV) has serine protease activity in its N-terminal region, which plays a crucial role in virus replication. This portion has also been reported to interact with not only its viral cofactor NS4A but also a number of host cellular proteins, which suggests a multi-functional feature of NS3. By means of yeast two-hybrid screening using an N-terminal region of NS3 as bait, we molecularly cloned a human cDNA encoding a portion of ELKS-δ, a member of a novel family of proteins that are involved in intracellular transport and secretory pathways. By using coimmunoprecipitation, GST pull-down, confocal microscopic and immunoelectron microscopic analyses, we demonstrated that full-length NS3 physically interacted with full-length ELKS-δ and its splicing variant ELKS-α, both in the absence and presence of NS4A, in cultured human cells, including Huh-7 cells harbouring HCV subgenomic RNA replicon. The degree of the binding to ELKS-δ varied with different sequences of the N-terminal 180 residues of NS3. Interestingly, NS3, either the full-length or the N-terminal fragments, enhanced secretion of secreted alkaline phosphatase (SEAP) from the cells and the increase in SEAP secretion correlated well with the degree of the binding between NS3 and ELKS-δ. Taken together, our results suggest the possibility that NS3 plays a role in modulating host cell functions such as intracellular transport and secretion through its binding to ELKS-δ and ELKS-α, which may facilitate the viral life cycle and/or mediate the pathogenesis of HCV.

INTRODUCTION

Hepatitis C virus (HCV) is the causative agent of non-A, non-B hepatitis (Choo *et al*., 1989). It has been estimated that more than 170 million individuals are infected with HCV worldwide, representing nearly 3% of the world's population (WHO, 1999). The majority of the patients remain chronically infected, suffering from chronic liver disorder, such as chronic hepatitis, liver cirrhosis and hepatocellular carcinoma (HCC).

HCV, an enveloped RNA virus, belongs to the genus *Hepacivirus* of the *Flaviviridae* family. The HCV genome is single-stranded, positive-sense RNA of approximately 9.6 kb, which contains a large open reading frame (ORF) flanked by the 5' and 3' untranslated regions (Reed & Rice, 2000). The ORF encodes a polyprotein of about 3,000 amino acids (aa), which is cleaved by the cellular signal peptidase and virally encoded two proteases into at least 10 mature proteins: core, envelope glycoprotein 1 (E1), E2, p7, nonstructural protein 2 (NS2), NS3, NS4A, NS4B, NS5A and NS5B (Hijikata *et al*., 1991, 1993).

NS3 is comprised of two domains, one possessing serine protease activity and the other RNA helicase activity, both of which are essential for virus replication. The protease domain resides in the N-terminal part of NS3 while the helicase domain in the C-terminal part. The NS3 enzymatic activities are modulated by NS4A, which forms a complex with NS3 to stabilize and localise it to perinuclear endoplasmic reticulum (ER) membranes (Reed & Rice, 2000; Wölk *et al*., 2000). NS3 also interacts with the other NS proteins, either directly or indirectly through host cell proteins, to form the viral replication complex (Aizaki *et al*., 2004).

The interactions between NS3 and cellular proteins have been studied to elucidate its role(s) in viral pathogenesis as well (Reed & Rice, 2000; Tellinghuisen & Rice, 2002). The helicase domain of NS3 was shown to interact with protein kinase A (PKA) (Borowski *et al*., 1999a; Aoubala *et al*.,

2001). It was also reported that NS3 served as substrates for protein kinase C (PKC) and inhibited PKC signalling via competition with its physiological substrates (Borowski *et al.*, 1999b). NS3 also binds to histone H2B and H4 (Borowski *et al.*, 1999c). The NS3 helicase domain was also shown to be essential for NS3 protein methylation by the protein arginine methyltransferase 1 (Rho *et al.*, 2001).

The studies on the NS3 serine protease domain demonstrated that it could transform NIH3T3 cells (Sakamuro *et al.*, 1995), rat fibroblast (Zemel *et al.*, 2001) and human liver cell line QSG7701 (He *et al.*, 2003), although the underlying mechanism(s) remains to be elucidated. Previously, we reported that the oncogenic properties of NS3 might involve an interaction with the tumour suppressor p53 (Ishido & Hotta, 1998; Muramatsu *et al.*, 1997). The protease domain of NS3 was reported also to bind to Sm-D1, a component of small nuclear ribonucleoprotein (snRNP) that is associated with autoimmune disease (Iwai *et al.*, 2003). A more recent study demonstrated that the protease domain of NS3 interacted with LMP7, a component of the immunoproteasome, and down-regulated the proteasome peptidase activity (Khu *et al.*, 2004).

To identify another possible cellular target(s) that interacts with the NS3 protease domain, we screened a human cDNA library by using a yeast two-hybrid system. We report here that NS3, through its protease domain, binds to ELKS-δ and its splice variant ELKS-α (Nakata *et al.*, 1999, 2002). Since a mouse homologue of ELKS-δ, namely Rab6-interacting protein 2B (Rab6IP2B), was reported to affect intracellular transport by binding to Rab6 (Monier *et al.*, 2002), we tested possible effects of NS3-ELKS-δ interaction on intracellular transport and secretory pathways using secreted alkaline phosphatase (SEAP) assay. We observed that NS3 augmented cellular secretion of SEAP and that the increase in SEAP secretion was proportional to the degree of the binding between NS3 and ELKS-δ. These results collectively suggest the possibility that NS3 affects intracellular transport and/or secretion pathways by interacting with ELKS-δ and ELKS-α.

METHODS

Plasmid construction. cDNA fragments encoding an N-terminal portion of NS3 (aa 1027 to 1208) were amplified from sera of HCV-1b-infected patients by reverse transcription-PCR, as described previously (Ogata *et al.*, 2002, 2003) with minor modifications using the primers NS3-F and NS3-181R (Supplementary Table A, which is available as Supplementary material in JGV Online). The amplified fragments were subcloned in-frame to the LexA DNA-binding domain of pHybLex/Zeo (Invitrogen) to generate pLex-NS3-H-31 and pLex-NS3-H-45 for expression in yeast. Frameshift mutants of bait (pLex-NS3-H-31-FS) and prey [pB42-ELKS-δ(787-1063)-FS] were generated by digesting the parental plasmids with *Eco*RI and *Bam*HI, respectively, followed by blunt-end formation and self-ligation. They served as negative controls. pB42-ATF6-α (Tong *et al.*, 2002) was also used as a negative control in this study.

A mammalian expression plasmid encoding Myc-tagged full-length NS3 [pcDNA3.1/NS3F(MKC1a)] was constructed by amplifying a cDNA fragment from pBSNS3/1027-1657 (Muramatsu *et al.*, 1997) using primers NS3/M/B and NS3FHindIII (Supplementary Table A), followed by subcloning into pcDNA3.1/*myc*-His(–)C (Invitrogen). Expression plasmids for chimeric forms of full-length NS3 were constructed, in which the N-terminal 180 residues are derived from clinical isolates, nos. 42, 45, H05-5 and H17-2 (Ogata *et al.*, 2002, 2003; GenBank accession nos. AB072084, AB072086, AB072048 and AB072055, respectively), while the C-terminal 451 residues being derived from MKC1a (GenBank accession no. D45172). These plasmids were designated pcDNA3.1/NS3(M-42) pcDNA3.1/NS3(M-45) pcDNA3.1/NS3(M-H05-5) and pcDNA3.1/NS3(M-H17-2).

A glutathione S-transferase (GST) fusion protein-expressing plasmid was also constructed. A vector plasmid, pcDNA3.1/GST, was constructed by introducing a 767-bp *Hinc*II fragment of

pGEXT-4T1 (Pharmacia) into *Eco*RI-digested, blunt-ended pcDNA3.1/*myc*-His(-)C. The full-length NS3-coding region of MKC1a was subcloned in-frame to pcDNA3.1/GST to generate pcDNA3.1/GST-NS3. pBS-GST-NS4B-F (Tong *et al*., 2002) and pBS-GST-NS5A-F (Taguchi *et al*., 2004) served as negative controls in this study.

Expression plasmids for FLAG-tagged, full-length ELKS-δ and ELKS-α were constructed. cDNA fragments of 3889-bp and 3834-bp encoding N-terminally deleted ELKS-δ and ELKS-α, respectively, were obtained by digesting pDR2-ELKS-δ and pDR2-ELKS-α (kind gifts from Dr. M. Emi, Institute of Gerontology, Nippon Medical School, Kawasaki, Kanagawa, Japan) with *Bam*HI and *Xba*I, and subcloned into pcDNA3.1/N-FLAG vector (Tong *et al*., 2002). Subsequently, a 718-bp sequence of ELKS-δ or ELKS-α (from the ATG initiation codon to the *Bam*HI site) was amplified by PCR from pDR2-ELKS-δ or pDR2-ELKS-α using the primers ELKS-F and ELKS-303R (Supplementary Table A), and subcloned into the above plasmids. The resultant plasmids were designated pcDNA3.1/N-FLAG-ELKS-δ and pcDNA3.1/N-FLAG-ELKS-α. Also, various deletion mutants of ELKS-δ were constructed by PCR using appropriate sets of primers (Supplementary Table A), followed by subcloning into the expression vector.

Yeast two-hybrid screening. Yeast two-hybrid screening was performed using Hybrid Hunter Kit (Invitrogen) and a human cDNA library, as reported previously with some modifications (Tong *et al*, 2002). In brief, an L40 strain carrying pLex-NS3-H31 was transformed with pYESTrp cDNA library prepared from HeLa cells (Invitrogen). Transformants were screened for growth on YC-WHUKZ300 plates lacking tryptophan, histidine, uracil and lysine but containing Zeocin. Resultant colonies were tested for β-galactosidase (β-Gal) activity according to the manufacturer's protocol.

Cell culture and protein expression. Vaccinia virus T7 hybrid expression was performed as reported previously (Muramatsu *et al*., 1997). In brief, HeLa cells were inoculated with recombinant vaccinia virus expressing T7 RNA polymerase (vTF7-3). After virus adsorption for 1 h, the cells were transfected with expression plasmids using Lipofectin (Invitrogen) and incubated overnight. The cells were then analysed for the possible protein-protein interaction (see below). For immunofluorescence and SEAP secretion assay, a plasmid-based expression method was employed with Fugene 6 transfection reagent (Roche). The cells were then incubated for 48 h before the analysis.

A Huh-7 cell line stably harbouring HCV subgenomic RNA replicon was prepared as previously described (Lohmann *et al.*, 2001; Taguchi *et al.*, 2004; Takigawa *et al.*, 2004), using pFK2884Gly (a kind gift from Dr. R. Bartenschlager, University of Heidelberg, Heidelberg, Germany). A cured Huh-7 cell line was prepared by maintaining the stable HCV replicon-harbouring cell line in the presence of alpha interferon (1,000 I.U./ml) for 1 month.

Double-staining immunofluorescence. Cells expressing Myc-tagged NS3 and FLAG-tagged ELKS-δ were fixed with 4% paraformaldehyde at room temperature for 15 min and permeabilized with 100% methanol at -20°C for 3 min. The cells were then blocked with 5% normal donkey serum for 1 h at room temperature. Primary antibodies used were anti-Myc mouse monoclonal antibody (Santa Cruz Biotech., Santa Cruz, CA, USA) and anti-FLAG rabbit polyclonal antibody (Sigma). FITC-conjugated goat anti mouse IgG (MBL, Nagoya, Japan) and Cy3-conjugated donkey anti-rabbit IgG (Chemicon) were used as secondary antibodies. The stained cells were observed with a laser scanning confocal microscope (LSM510 ver. 3.0, Carl Zeiss) or a fluorescence microscope (BX51, Olympus) attached to a DP70 CCD camera.

Immunoelectron microscopy. Cells expressing Myc-tagged NS3 and FLAG-tagged ELKS-δ were fixed with 4% paraformaldehyde and 0.2% glutaraldehyde for 30 min at room temperature. After being washed with phosphate-buffered saline (PBS), the cells were centrifuged at 1,500 rpm for 5 min. The cell pellet was dehydrated in a series of 70%, 80% and 90% ethanol, embedded in LR White resin (London Resin Co., Ltd., Berkshire), and kept at –20°C for 2 days to facilitate resin polymerisation. After ultrathin sectioning, the samples were etched in 3% H_2O_2 for 5 min at room temperature and washed with PBS. For labelling, sections were incubated with anti-Myc mouse monoclonal antibody and anti-FLAG rabbit antiserum for 1h. After being rinsed with PBS, the sections were incubated with goat anti-mouse IgG and goat anti-rabbit IgG conjugated with 5-nm and 10-nm gold (Sigma), respectively, for 1 h. The sections were post-stained with uranyl acetate and lead citrate, and observed under a transmission electron microscope (JEM 1200EX, JOEL).

Coimmunoprecipitation. Cells expressing Myc-tagged NS3 and FLAG-tagged ELKS-δ or ELKS-α were lysed in ice-cold RIPA buffer (1×PBS, 1% Nonidet P-40, 0.5% sodium deoxycholate, 0.1% SDS) with freshly added protease inhibitors (PMSF and aprotinin). The lysates were centrifuged at 10,000 × g for 10 min at 4°C and the supernatants were mixed with 0.25 μg of normal rabbit IgG and 20 μl of protein G-agarose beads (Pharmacia) at 4°C for 30 min to eliminate non-specific binding. The precleared lysates were incubated with anti-Myc rabbit polyclonal antibody for 1 h at 4°C, followed by incubation with 20 μl of protein G-agarose beads for another 1 h. After being washed five times with ice-cold RIPA buffer, the immunoprecipitates were analysed by immunoblotting, as described below.

Immunoblotting. Samples were subjected to SDS-polyacrylamide gel electrophoresis and electrophoretically blotted onto a polyvinylidene fluoride membrane (Immobilon-P, Millipore). After being blocked in PBS containing 5% skim milk, the membranes were incubated with anti-FLAG or anti-Myc mouse monoclonal antibody for 1 h. The membranes were then incubated with

peroxidase-labelled goat anti-mouse IgG (MBL) for 1 h. After being washed three times, the protein bands were visualized by an enhanced chemiluminescence method (ECL; Amersham Biosciences). Densitometric analysis was performed using a publicly available software (tnimage-3.3.14; http://brneurosci.org/tnimage.html).

GST-pull down assay. Lysates were prepared from the cells transiently expressing GST-tagged NS3 and FLAG-tagged ELKS-δ or ELKS-α. The lysates were mixed with 20 μl of glutathione-conjugated Sepharose 4B beads at 4°C for 90 min. The beads were washed five times with ice-cold RIPA buffer and subjected to immunoblot analysis using anti-FLAG antibody. To verify a comparable amount of the proteins in each sample, the lysates were directly (without pull-down) subjected to immunoblotting.

SEAP secretion assay. SEAP secretion assay was performed to measure a possible effect of NS3 on the secretory pathway. SEAP is a genetically engineered secreted form of alkaline phosphatase (Cullen & Malim, 1992) and the SEAP secretion assay has been widely used to monitor cellular secretory function including Rab6-mediated intracellular transport (Echard *et al.,* 2000; Martinez *et al.*, 1994). HeLa cells were transiently transfected with 200 ng of a pcDNA3.1-derived NS3 expression plasmid, 50 ng of pSEAP2-Control (BD Biosciences) and 1 ng of pRL-SV40 (Promega), either in the presence or absence of 200 ng of pcDNA3.1/N-Flag-ELKS-δ. pRL-SV40 was used to express *Renilla* luciferase as an internal control. After 48 h, culture medium was collected for SEAP secretion assay, while the cells were processed for *Renilla* luciferase assay. SEAP activities were measured using SEAP Reporter Gene Assay (Roche) and *Renilla* luciferase activities measured using *Renilla* Luciferase Assay System (Promega), according to the manufacturers' instructions. SEAP activities in each sample were normalized against *Renilla* luciferase activities. Since pSEAP2-Control and pRL-SV40 use the same SV40 early promoter, marginal effect of NS3

on the promoter activity (an increase by ~20%, as determined by *Renilla* luciferase activity) is nullified and the effect on SEAP secretion can be determined by this assay.

RESULTS

Identification of ELKS-δ as an NS3-interacting protein by yeast two-hybrid assay. To identify a human protein(s) that physically interacts with NS3 protease domain (aa 1027 to 1208) (Fig. 1A), ←Fig. 1 the L40 yeast strain harbouring pLex-NS3-H-31 was transformed with the pYESTrp-based HeLa cDNA library and screened for growth on YC-WHUKZ300 selection plates. Out of 5.8×10^7 primary transformants screened, 260 colonies grew on the selection plates. Further screening for β-Gal activity identified a clone that showed strong reaction. DNA sequence analysis revealed that the yeast clone carried a pYESTrp-driven sequence that completely matched the sequence for a C-terminal portion of ELKS-δ (GenBank accession no. AB053470) (Nakata *et al*., 2002). The cloned cDNA fragment was designated ELKS-δ(787-1063).

Specificity of the interaction between the NS3 and ELKS-δ(787-1063) was tested by transfecting the parental (naïve) L40 strain with various combinations of the expression plasmids, including two different NS3 sequences (H-31 and H-45) and the frameshift mutants of NS3-H-31 and ELKS-δ(787-1063). The results demonstrated specific interaction between the NS3 protease domain and ELKS-δ(787-1063) in yeast (Fig. 1B).

NS3 interacts with ELKS-δ and its splice-variant ELKS-α in cultured human cells. The interaction between NS3 and ELKS-δ was further investigated in mammalian cells and specific interaction between the protease domain of NS3 and ELKS-δ(787-1063) was observed (data not shown). Moreover, full-length NS3 (aa 1027 to 1657) was shown to interact with ELKS-δ(787-1063) in HeLa cells (Fig. 2A, lane 2). We then narrowed down the region of ELKS-δ responsible ←Fig. 2 for the interaction with full-length NS3. C-terminal truncation of ELKS-δ up to aa 1008 did not

affect the interaction with NS3. However, further deletion up to aa 995 or aa 979 abolished the ability to interact with NS3. N-terminal truncation of the initial fragment up to aa 846 did not affect the interaction with NS3 while further deletion up to aa 876 or aa 886 completely abolished it. These results mapped a minimum NS3-interacting region somewhere between aa 846 and 1008 of ELKS-δ. Consistently, ELKS-δ(846-1008) interacted with NS3. Similar results were obtained using yeast two-hybrid system (data not shown).

Next, we tested interaction of full-length NS3 with full-length ELKS-δ and its splice-variant ELKS-α. GST pull-down analysis demonstrated that full-length NS3 interacted with full-length ELKS-δ and ELKS-α as well (Fig. 3A). Specificity of the interaction between NS3 and ELKS-δ was confirmed by demonstrating that neither NS4B nor NS5A of HCV bound to full-length ELKS-δ under the same experimental condition (Fig. 3B). Specific interaction between the two molecules was also confirmed by coimmunoprecipitation analysis, in which anti-FLAG antibody (directed against FLAG-tagged full-length ELKS-δ and ELKS-α) coimmunoprecipitated full-length NS3 (data not shown). ←Fig. 3

In order to determine whether NS3 interacts with ELKS proteins in the presence of the other HCV non-structural proteins, we expressed ELKS-δ and ELKS-α in Huh-7 cells harbouring HCV subgenomic RNA replicon, and subsequently immunoprecipitated NS3 using anti-NS3 polyclonal antibody. The result demonstrated that NS3 expressed in the context of HCV replication interacted with full-length ELKS-δ and ELKS-α in HCV RNA replicon-harbouring cells (Fig. 3C).

Sequence comparison between ELKS-δ and ELKS-α. The aa sequences of ELKS-δ and ELKS-α differ from each other in their C-termini due to alternative splicing (Fig. 4A). As shown above, a minimum region responsible for the interaction with NS3 was mapped between aa 846 and 1008 of ELKS-δ (see Fig. 2). Since full-length ELKS-α interacted with NS3 (see Fig. 3), we then ←Fig. 4

272 determined a minimum region of ELKS-α responsible for the interaction. Deletion mutational
273 analysis revealed that ELKS-α(747-948), but not ELKS-α(763-948), ELKS-α(791-948) or ELKS-
274 α(806-948), interacted with NS3 (Fig. 4B and 4C), suggesting that ELKS-α(747-948) is a
275 minimum region responsible for the interaction with NS3.
276
277 **NS3 colocalises with ELKS-δ in human cells.** We visualized the colocalisation of NS3 with
278 ELKS-δ in Huh-7 cells by double-staining immunofluorescence analysis. When coexpressed in
279 Huh-7 cells by the plasmid-based expression methods, full-length NS3 colocalised with full-length
280 ELKS-δ in the cytoplasm, both in the absence (Fig. 5A) and presence of NS4A (Fig. 5B). ←Fig. 5
281 Colocalisation of NS3 with ELKS-δ was observed also in HCV RNA replicon-harbouring cells
282 (Fig. 5C).
283
284 Immunoelectron microscopic analysis also demonstrated colocalisation of full-length NS3 with
285 full-length ELKS-δ in close proximity to the ER membranes in the perinuclear region (Fig. 5D).
286
287 **NS3 differentially interacts with ELKS-δ in an NS3 sequence-dependent manner.** A
288 considerable degree of sequence variation has been observed in the N-terminal 180 residues of NS3
289 (Ogata *et al.*, 2002, 2003). We performed experiments to determine whether or not interaction with
290 ELKS-δ varies with different NS3 sequences. We first used 198-residue fragments of NS3
291 obtained from four patients (nos. 42, 45, H05-5 and H17-2) and found that the degree of the
292 interaction with ELKS-δ varied with different sequences (data not shown). Next, we tested full-
293 length NS3 sequences of five different isolates, a parental strain (MKC1a) and four chimeric forms
294 (M-42, M-45, M-H05-5 and M-H17-2), which differ with each other by at most 10 residues within
295 the N-terminal 180 residues, with the remaining C-terminal 451 residues being shared in common
296 by all five isolates. These full-length forms of NS3 were each expressed with full-length ELKS-δ
297 and their interaction examined. Consistent with the result obtained with the 198-residue fragments,

the degree of the interaction between full-length NS3 and ELKS-δ varied with different NS3 sequences, with M-42 and M-45 showing stronger interaction than the others while M-H05-5 showing the weakest (Fig. 6A and 6B). Sequence alignment of the N-terminal 180 residues of NS3 ←Fig. 6 is shown in Fig. 6C. Five residues (Val-1044, Leu-1106, Ala-1176, Val-1179 and Ile-1196) are unique to M-H05-5. Based on this sequence alignment alone, however, it was difficult to draw a conclusion as to which residue(s) affects most significantly the interaction with ELKS-δ.

When NS4A was coexpressed, the interaction between NS3 and ELKS-δ became weaker, though still detectable, and the NS3 sequence-dependent difference in the interaction with ELKS-δ was not clearly observed (data not shown).

NS3 enhances SEAP secretion from the cell possibly through its interaction with ELKS-δ. The binding domain of Rab6IP2, a murine homologue of ELKS-δ, was reported to affect the endosome-to-Golgi retrograde transport pathway through its binding to Rab6 (Monier *et al.*, 2002). Also, CAST and ERC proteins, rat homologues of the ELKS protein family, were implicated in the modulation of neurotransmitter secretion (Deguchi-Tawarada *et al.*, 2004; Ohtsuka *et al.*, 2002; Wang *et al.*, 2002). We assumed that NS3 might affect the possible function of ELKS-δ and/or its splice-variant(s), modulating intracellular transport and secretory function. Therefore, we performed SEAP assay. The results demonstrated that SEAP secretion was significantly enhanced by NS3 of three isolates (MKC1a, M-42 and M-45), especially when ELKS-δ was ectopically expressed (Fig. 7A). In this connection, we assume that endogenous ELKS-δ was also expressed, ←Fig. 7 though to a lesser extent. On the other hand, NS3 of the other isolates (M-H-05-5 and M-H17-2) did not enhance SEAP secretion in the absence of ectopic ELKS-δ while a mild enhancement by NS3 of M-H17-2 was observed when ELKS-δ was ectopically expressed. Interestingly, the degree of the interaction between NS3 and ELKS-δ correlated well to the level of the increase in SEAP secretion (Fig. 7B). Moreover, SEAP secretion was enhanced in HCV RNA replicon-harbouring

Huh-7 cells compared to HCV RNA-negative Huh-7 cells that had been cured by interferon treatment (Fig. 7C). These results strongly suggest that NS3 affects the cellular secretory pathway by interacting with ELKS-δ and ELKS-α.

DISCUSSION

In the present study we demonstrated that an N-terminal protease domain of HCV NS3 physically interacted with ELKS-δ and ELKS-α in yeast and cultured human cells (Figs. 1 to 5). The interaction was observed also in the presence of NS4A (Fig. 5B) and in HCV RNA replicon-harbouring cells (Figs. 3C and 5C), where NS3 is expressed in the context of HCV RNA replication to form viral replication complex in a unique membranous structure (Aizaki *et al.*, 2004). It was also demonstrated that the degree of the interaction with ELKS-δ varied with different NS3 sequences (Fig. 6). The N-terminal 180 residues of M-42 and M-45, which bound to ELKS-δ more efficiently than did M-H05-5, were derived from HCV isolates obtained from patients without HCC, whereas those of M-H05-5 and M-H17-2 from patients with HCC (Ogata et al., 2002, 2003). It is intriguing to speculate that certain NS3 sequences with less preference for ELKS-δ binding are more likely to interact with, and modulate the function of, another host factor(s), such as p53 (L. Deng *et al.*, unpublished data; Ishido & Hotta, 1998; Muramatsu *et al.*, 1997), thus facilitating the development of HCC. However, with the limited number of samples tested, it was difficult to draw a conclusion about the correlation between the NS3-ELKS-δ interaction and certain clinical symptoms including HCC.

ELKS was initially identified as a protein fused to RET proto-oncogene product in human papillary thyroid carcinoma (Nakata *et al.*, 1999). Four other splice-variants of the ELKS protein family were subsequently identified and designated ELKS-β, -γ, -δ and -ε, with the prototype isoform being renamed as ELKS-α (Nakata *et al.*, 2002). A number of related proteins highly homologous to the ELKS proteins were identified in rat, named CAST (CAST1, CAST2α and CAST2β)

(Deguchi-Tawarada *et al.*, 2004; Ohtsuka *et al.*, 2002) and ERC (ERC1a, ERC1b and ERC2) (Wang *et al.*, 2002). Another research group discovered two related mouse proteins that specifically interacted with a small GTPase protein Rab6 and, therefore, the proteins were named Rab6IP2A and Rab6IP2B (Monier *et al.*, 2002). Sequence alignment has revealed that ELKS, CAST, ERC and Rab6IP2 are the ortholog members of the same protein family in human, rat and mouse. Their expression profiles in the body differ with different isoforms, with ELKS-α, CAST2α, Rab6IP2A, ERC1b and ERC2 being expressed only in the brain, while ELKS-δ, Rab6IP2B and ERC1a being expressed ubiquitously outside of the brain (Nakata *et al.*, 2002; Deguchi-Tawarada *et al.*, 2004). In the present study we have mapped minimum NS3-binding sequences to the regions spanning from aa 846 to 1008 of ELKS-δ (Fig. 2) and from aa 747 to 948 of ELKS-α (Fig. 4). Since the sequence of ELKS-δ from aa 846 to 1008 completely matches that of the corresponding region of ELKS-ε (aa 874 to 1036), ELKS-ε is most likely to interact with NS3. On the other hand, when compared with the minimum NS3-binding sequence of ELKS-α (aa 747 to 948), the corresponding region of ELKS-β (aa 747 to 992) and ELKS–γ (aa 475 to 720) have an identical insertion of 44 residues between positions 805 and 806 of ELKS-α. At present, we do not know whether or not this insertion affects the interaction with NS3.

Rab6IP2A and Rab6IP2B were reported to partially inhibit the endosome-to-Golgi retrograde transport pathway through their binding to Rab6 (Monier *et al.*, 2002). Similarly, CAST and ERC proteins were postulated to modulate neurotransmitter release through interacting with RIMs that are localised in the presynaptic active zone and involved in exocytosis of neurotransmitters in Rab3-dependent manner (Deguchi-Tawarada *et al.*, 2004; Ohtsuka *et al.*, 2002; Wang *et al.*, 2002). It is thus possible that certain ELKS-binding proteins, including viral products, affect intracellular transport and secretory pathways, either positively or negatively, by counteracting or augmenting the function of ELKS proteins. Indeed, we observed that HCV NS3 enhanced SEAP secretion from the cells. Interestingly, the degree of the secretion enhancement correlated well with the

degree of binding between NS3 and ELKS-δ (Fig. 7B). It has been reported that Rab6 is expressed in hepatocytes, playing an important role in regulating intracellular transport at the level of the Golgi complex (Feldmann *et al.*, 1995). Also, ELKS-δ and its mouse counterpart Rab6IP2B are expressed ubiquitously in the body (Monier *et al.*, 2002; Nakata *et al.*, 2002). Therefore, it is reasonable to assume that, even in a natural setting, *i.e.*, in HCV-infected hepatocytes *in vivo*, NS3 interacts with ELKS-δ to modulate Rab6-dependent intracellular transport and secretory pathways, thereby facilitating intracellular transport of viral components so that the virion formation takes place efficiently. However, the precise role for this interaction in the viral life cycle and/or viral pathogenesis is still unknown and awaits further investigation.

We observed enhanced SEAP secretion from Huh-7 cells harbouring HCV subgenomic RNA replicon, compared with the secretion from parental Huh-7 cells and interferon-treated cured cells (Fig 7C). In this connection, it was recently reported that the rate of MHC class I traffic to the cell surface was inhibited in Huh-7 cells harbouring HCV subgenomic RNA replicon and that the inhibition was mediated probably by the NS4A/B precursor protein (Konan *et al.*, 2003). At present, we do not know the reason for the apparent discrepancy between their results (inhibited MHC class I traffic) and ours (enhanced SEAP secretion) in HCV RNA replicon-harbouring cells. It is possible that these events occur through different mechanisms, which selectively modulate intracellular transport and secretion of a particular protein(s).

Recently, Ducut Sigala *et al.* (2004) identified ELKS-α as an essential regulatory subunit of the IκB kinase complex, a modulator of the nuclear factor-kappa B (NF-κB) transcription factor activation. They described that ELKS-α was involved in induced expression of NF-κB target genes including proinflammatory ones, and also in establishing cellular anti-apoptotic status in response to tumour necrosis factor-α. These findings, together with our present observations, imply the possibility that NS3, through its interaction with ELKS-δ and ELKS-α, modulates NF-

κB activation, thereby facilitating HCV pathogenesis, such as inflammation and tumour formation in the liver. Further studies are needed to elucidate the issues.

ACKNOWLEDGEMENTS

The authors are grateful to Dr. M. Emi (Institute of Gerontology, Nippon Medical School, Kawasaki, Kanagawa, Japan) for providing the plasmids pDR2-ELKS-δ (p14) and pDR2-ELKS-α (p32) Thanks are also due to Dr. R. Bartenschlager (University of Heidelberg, Heidelberg, Heidelberg, Germany) for providing an HCV subgenomic RNA replicon (pFK5B2884Gly). This work was supported in part by grants-in-aid for Scientific Research from Ministry of Education, Culture, Sports, Science and Technology, Japan, and the Japan Society for the Promotion of Science.

REFERENCES

Aizaki, H., Lee, K. J., Sung, V. M., Ishiko, H. & Lai, M. M. (2004). Characterization of the hepatitis C virus RNA replication complex associated with lipid rafts. *Virology* **324,** 450-461.

Aoubala, M., Holt, J., Clegg, R. A., Rowlands, D. J. & Harris, M. (2001). The inhibition of cAMP-dependent protein kinase by full-length hepatitis C virus NS3/4A complex is due to ATP hydrolysis. *J Gen Virol* **82,** 1637-1646.

Borowski, P., Heiland, M., Feucht, H. & Laufs, R. (1999a). Characterisation of non-structural protein 3 of hepatitis C virus as modulator of protein phosphorylation mediated by PKA and PKC: evidences for action on the level of substrate and enzyme. *Arch Virol* **144,** 687-701.

Borowski, P., Schulze zur Wiesch, J., Resch, K., Feucht, H., Laufs, R. & Schmitz, H. (1999b). Protein kinase C recognizes the protein kinase A-binding motif of nonstructural protein 3 of hepatitis C virus. *J Biol Chem* **274,** 30722-30728.

Borowski, P., Kühl, R., Laufs, R., Schulze zur Wiesch, J. & Heiland, M. (1999c). Identification and characterization of a histone binding site of the non-structural protein 3 of hepatitis C virus. *J Clin Virol* **13,** 61-69.

Choo, Q. L., Kuo, G., Weiner, A. J., Overby, L. R., Bradley, D. W. & Houghton, M. (1989). Isolation of a cDNA clone derived from a blood-borne non-A, non-B viral hepatitis genome. *Science* **244,** 359-362.

Cullen, B. R. & Malim, M. H. (1992). Secreted placental alkaline phosphatase as a eukaryotic reporter gene. *Methods Enzymol* **216,** 362-368.

Deguchi-Tawarada, M., Inoue, E., Takao-Rikitsu, E., Inoue, M., Ohtsuka, T. & Takai, Y. (2004). CAST2: identification and characterization of a protein structurally related to the presynaptic cytomatrix CAST. *Genes Cells* **9,** 15-23.

Ducut Sigala, J. L., Bottero, V., Young, D. B., Shevchenko, A., Mercurio, F. & Verma, I. M. (2004). Activation of transcription factor NF-κB requires ELKS, and IκB kinase regulatory subunit. *Science* **304,** 1963-1967.

Echard, A., Opdam, F. J., de Leeuw, H. J., Jollivet, F., Savelkoul, P., Hendriks, W., Voorgerg, J., Goud, B. & Fransen, J. A. (2000). Alternative splicing of the human Rab6A gene generates two close but functionally different isoforms. *Mol Biol Cell* **11,** 3819-3833.

Feldmann, G., Durand-Schneider, A. M. & Goud, B. (1995). Behaviour of the small GTP-binding protein rab6 in the liver of normal rats and rats presenting an acute inflammatory reaction. *Biol Cell* **83,** 121-125.

He, Q. Q., Cheng, R. X., Sun, Y., Feng, D. Y., Chen, Z. C. & Zeng, H. (2003). Hepatocyte transformation and tumor development induced by hepatitis C virus NS3 C-terminal deleted protein. *World J Gastroenterol* **9,** 474-478.

Hijikata, M., Kato, N., Ootsuyama, Y., Nakagawa, M. & Shimotohno, K. (1991). Gene mapping of the putative structural region of the hepatitis C virus genome by in vitro processing analysis. *Proc Natl Acad Sci USA* **88,** 5547-5551.

Hijikata, M., Mizushima, H., Tanji, Y., Komoda, Y., Hirowatari, Y., Akagi, T., Kato, N., Kimura, K. & Shimotohno, K. (1993). Proteolytic processing and membrane association of putative nonstructural proteins of hepatitis C virus. *Proc Natl Acad Sci USA* **90,** 10773-10777.

Ishido, S. & Hotta, H. (1998). Complex formation of the nonstructural protein 3 of hepatitis C virus with the p53 tumor suppressor. *FEBS Lett* **438,** 258-262.

Iwai, A., Hasumura, Y., Nojima, T. & Takegami, T. (2003). Hepatitis C virus nonstructural protein NS3 binds to Sm-D1, a small nuclear ribonucleoprotein associated with autoimmune disease. *Microbiol Immunol* **47,** 601-611.

Konan, K. V., Giddings, T. H. Jr., Ikeda, M., Li, K., Lemon, S. M. & Kirkegaard, K. (2003). Nonstructural protein precursor NS4A/B from hepatitis C virus alters function and ultrastructure of host secretory apparatus. *J Virol* **77,** 7843-7855.

Khu, Y. L., Tan, Y. J., Lim, S. G., Hong, W. & Goh, P. Y. (2004). Hepatitis C virus non-structural protein NS3 interacts with LMP7, a component of the immunoproteasome, and affects its proteasome activity. *Biochem J* **384,** 401-409.

Lohmann, V., Körner, F., Dobierzewska, A. & Bartenschlager, R. (2001). Mutations in hepatitis C virus RNAs conferring cell culture adaptation. *J Virol* **75,** 1437-1449.

Martinez, O., Schmidt, A., Salamero, J., Hoflack, B., Roa, M. & Goud, B. (1994). The small GTP-binding protein rab6 functions in intra-Golgi transport. *J Cell Biol* **127,** 1575-1588.

Monier, S., Jollivet, F., Janoueix-Lerosey, I., Johannes, L. & Goud, B. (2002). Characterization of novel Rab6-interacting proteins involved in endosome-to-TGN transport. *Traffic* **3,** 289-297.

Muramatsu, S., Ishido, S., Fujita, T., Itoh, M. & Hotta, H. (1997). Nuclear localization of the NS3 protein of hepatitis C virus and factors affecting the localization. *J Virol* **71,** 4954-4961.

Nakata, T., Kitamura, Y., Shimizu, K., Tanaka, S., Fujimori, M., Yokoyama, S., Ito, K. & Emi, M. (1999). Fusion of a novel gene, *ELKS*, to *RET* due to translocation t(10;12)(q11;p13) in a papillary thyroid carcinoma. *Genes Chromosomes Cancer* **25,** 97-103.

Nakata, T., Yokota, T., Emi, M. & Minami, S. (2002). Differential expression of multiple isoforms of the *ELKS* mRNAs involved in a papillary thyroid carcinoma. *Genes Chromosomes Cancer* **35,** 30-37.

Ogata, S., Ku, Y., Yoon, S., Makino, S., Nagano-Fujii, M. & Hotta, H. (2002). Correlation between secondary structure of an amino-terminal portion of the nonstructural protein 3 (NS3) of hepatitis C virus and development of hepatocellular carcinoma. *Microbiol Immunol* **46,** 549-554.

Ogata, S., Florese, R. H., Nagano-Fujii, M., Hidajat, R., Deng, L., Ku, Y., Yoon, S., Saito, T., Kawata, S. & Hotta, H. (2003). Identification of hepatitis C virus (HCV) subtype 1b strains that are highly, or only weakly, associated with hepatocellular carcinoma on the basis of the secondary structure of an amino-terminal portion of the HCV NS3 protein. *J Clin Microbiol* **41**, 2835-2841.

Ohtsuka, T., Takao-Rikitsu, E., Inoue, E., Inoue, M., Takeuchi, M., Matsubara, K., Deguchi-Tawarada, M., Satoh, K., Morimoto, K., Nakanishi, H. & Takai, Y. (2002). CAST: a novel protein of the cytomatrix at the active zone of synapses that forms a ternary complex with RIM1

and Munc13-1. *J Cell Biol* **158,** 577-590.

Reed, K. E. & Rice, C. M. (2000). Overview of hepatitis C virus genome structure, polyprotein processing, and protein properties. *Curr Top Microbiol Immunol* **242,** 55-84.

Rho, J., Choi, S., Seong, Y., Choi, J. & Im, D. (2001). The arginine-1493 residue in QRRGRTGR1493G motif IV of the hepatitis C virus NS3 helicase domain is essential for NS3 protein methylation by the protein arginine methyltransferase 1. *J Virol* **75,** 8031-8044.

Sakamuro, D., Furukawa, T. & Takegami, T. (1995). Hepatitis C virus nonstructural protein NS3 transforms NIH 3T3 cells. *J Virol* **69,** 3893-3896.

Taguchi, T., Nagano-Fujii, M., Akutsu, M., Kadoya, H., Ohgimoto, S., Ishido, S. & Hotta, H. (2004). Hepatitis C virus NS5A protein interacts with 2',5'-oligoadenylate synthetase and inhibits antiviral activity of IFN in an IFN sensitivity-determining region-independent manner. *J Gen Virol* **85,** 959-969.

Takigawa, Y., Nagano-Fujii, M., Deng, L., Hidajat, R., Tanaka, M., Mizuta, H. & Hotta, H. (2004). Suppression of hepatitis C virus replicon by RNA interference directed against the NS3 and NS5B regions of the viral genome. *Microbiol Immunol* **48,** 591-598.

Tellinghuisen, T. L. & Rice, C. M. (2002). Interaction between hepatitis C virus proteins and host cell factors. *Curr Opin Microbiol* **5,** 419-427.

Tong, W. Y., Nagano-Fujii, M., Hidajat, R., Deng, L., Takigawa, Y. & Hotta, H. (2002). Physical interaction between hepatitis C virus NS4B protein and CREB-RP/ATF6β. *Biochem*

Biophys Res Commun **299,** 366-372.

Wang, Y., Liu, X., Biederer, T. & Südhof, T. C. (2002). A family of RIM-binding proteins regulated by alternative splicing: Implications for the genesis of synaptic active zones. *Proc Natl Acad Sci USA* **99,** 14464-14469.

Wölk, B., Sansonno, D., Kräusslich, H. G., Dammacco, F., Rice, C. M., Blum, H. E. & Moradpour, D. (2000). Subcellular locacalization, stability, and *trans*-cleavage competence of the hepatitis C virus NS3-NS4A complex expressed in tetracycline-regulated cell lines. *J Virol* **74,** 2293-2304.

World Health Organization. (1999). Hepatitis C – global prevalence (update). *Weekly Epidemiol Rec* **74,** 425-427.

Zemel, R., Gerechet, S., Greif, H., Bachmatove, L., Birk, Y., Golan-Goldhirsh, A., Kunin, M., Berdichevsky, Y., Benhar, I. & Tur-Kaspa, R. (2001). Cell transformation induced by hepatitis C virus NS3 serine protease. *J Viral Hepat* 8, 96-102.

LEGENDS TO FIGURES

Fig. 1. Identification of ELKS-δ as an NS3-binding protein by yeast two-hybrid assay. (A) Schematic diagram of the HCV genome. An N-terminal serine protease domain of NS3 (aa 1027 to 1208) used as 'bait' is also depicted. (B) A representative result showing specific interaction between the NS3 protease domain and ELKS-δ(787-1063). The L-40 yeast strain cotransfected with the indicated plasmids was grown on tryptophan-deficient media containing antibiotic Zeocin and subsequently assayed for β-galactosidase (β-Gal) activity. Blue colour development within 30 min indicates strong interaction between the two proteins of interest.

Fig. 2. Determination of a minimal region of ELKS-δ required for interaction with full-length NS3 in cultured human cells. (A) A series of deletion mutants of FLAG-tagged ELKS-δ were expressed by the vaccinia-T7 hybrid expression method in HeLa cells without (lanes of odd numbers) or with Myc-tagged full-length NS3 (lanes of even numbers). Cell lysates were immunoprecipitated using anti-Myc antibody and probed by immunoblotting using anti-FLAG antibody (upper panel). The lysates were directly (without being immunoprecipitated with anti-Myc antibody) probed with anti-FLAG antibody to verify comparable degrees of expression of the ELKS-δ mutants (middle panel). Efficient immunoprecipitation of Myc-tagged NS3 with anti-Myc antibody was also verified (lower panel). (B) Schematic diagram of the various deletion mutants of ELKS-δ. ++, strong interaction; –, no interaction.

Fig. 3. Full-length ELKS-δ and ELKS-α interact with full-length NS3 in cultured human cells. (A) FLAG-tagged full-length ELKS-δ (lanes 1 and 4), full-length ELKS-α (lanes 2 and 5) and a deletion mutant, ELKS-δ(787-1063) (lanes 3 and 6), were coexpressed in HeLa cells with GST (lanes 1 to 3) or full-length NS3 fused to GST (lanes 4 to 6). Cell lysates were pulled down with glutathione beads and probed with anti-FLAG antibody (upper panel). The lysates were directly

(without being pulled down) probed with anti-FLAG antibody to confirm expression of ELKS-δ or ELKS-α (middle panel). Efficient pull-down was also verified (lower panel). (B) FLAG-tagged full-length ELKS-δ was coexpressed in HeLa cells with empty vector (lane 2), GST (lane 3), GST-tagged full-length NS3 (lane 4), full-length NS4B (lane 5) and full-length NS5A (lane 6). Cells lysates were pulled down by glutathione beads and probed with anti-FLAG antibody (upper panel). The lysates were directly probed with anti-FLAG antibody to confirm ELKS-δ expression (middle panel). Efficient pull-down was also verified (lower panel). (C) FLAG-tagged full-length ELKS-δ (lanes 2 and 6), full-length ELKS-α (lanes 3 and 7) and a deletion mutant, ELKS-δ(787-1063) (lanes 4 and 8), were expressed in Huh-7 cells harbouring HCV RNA replicon (lanes 5 to 8) and the parental Huh-7 as a control (lanes 1 to 4). Cell lysates were immunoprecipitated with anti-NS3 polyclonal antibody and probed with anti-FLAG antibody (upper panel). Expression of ELKS-δ and ELKS-α (middle panel) and efficient immunoprecipitation of NS3 (lower panel) were also verified.

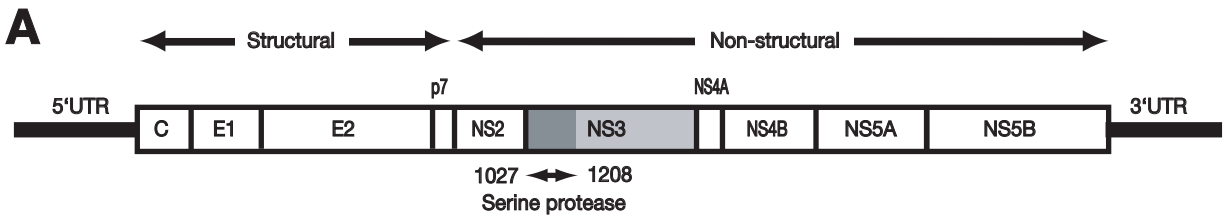
Fig. 4. Sequence comparison of C-terminal portions of ELKS-δ and ELKS-α. (A) Sequence alignment of a C-terminal portion of ELKS-δ and ELKS-α. Asterisks indicate identical residues. Hyphens indicate missing residues when compared to the other isoform. Underlined (aa 846 to 1008) is a minimum portion of ELKS-δ required for interaction with NS3 (see Fig. 2). (B) A series of deletion mutants of FLAG-tagged ELKS-α were expressed without (lanes of odd numbers) or with Myc-tagged full-length NS3 (lanes of even numbers). ELKS-δ(787-1063) (lanes 3 and 4) served as a positive control. Cell lysates were immunoprecipitated using anti-Myc antibody and probed with anti-FLAG antibody (upper panel). The lysates were directly probed with anti-FLAG antibody to confirm expression of the ELKS-α mutants (middle panel). Efficient immunoprecipitation of NS3 was also verified (lower panel). (C) Schematic diagram of the ELKS-α deletion mutants. +, moderate interaction (weaker than ELKS-δ[787-1063]) ; –, no interaction.

Fig. 5. Full-length ELKS-δ colocalises with full-length NS3 in cultured human cells. FLAG-tagged full-length ELKS-δ was coexpressed in Huh-7 cells with Myc-tagged full-length NS3 in the absence (A) and presence of NS4A (B), or in HCV RNA replicon-harbouring Huh-7 cells (C), and were examined by double-staining immunofluorescence analysis. The orange colour in the cytoplasm observed in the merged pictures indicates colocalisation of the two proteins. (D) FLAG-tagged full-length ELKS-δ was coexpressed with Myc-tagged full-length NS3 in HeLa cells. The cells were simultaneously stained with antibodies to Myc (5 nm diameter gold particles, thin arrows) and FLAG (10 nm diameter gold particles, thick arrows). Close proximity between both particles indicates tight interaction between the two proteins.

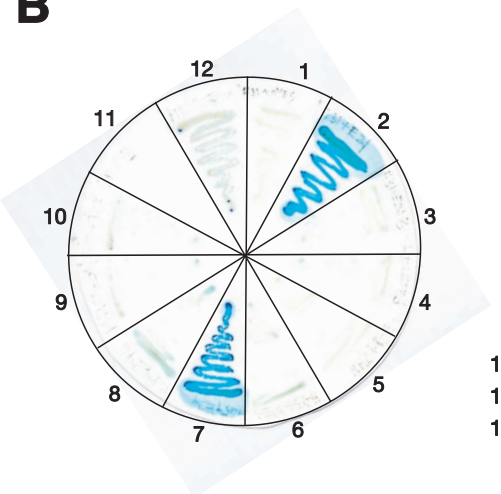
Fig. 6. NS3 interacts with ELKS-δ in a sequence-dependent manner. (A) FLAG-tagged full-length ELKS-δ was coexpressed with Myc-tagged full-length NS3 of different sequences by the plasmid based expression method in HeLa cells. Cell lysates were immunoprecipitated using anti-Myc antibody and probed with anti-FLAG antibody (upper panel). The lysates were directly probed with anti-FLAG antibody to confirm ELKS-δ expression (middle panel). Efficient immunoprecipitation of NS3 was also verified (lower panel). (B) The intensities of the bands of ELKS-δ that had been coimmunoprecipitated with NS3 were quantitated using a software (tnimage-3.3.14) and normalized to ELKS-δ expression level. Mean ± S.D. obtained from two independent experiments are shown. *, $P<0.05$, compared with M-H05-5; †, $P<0.05$, compared with M-H17-2. (C) Sequence alignment of the N-terminal 180 residues of NS3 of different isolates. Asterisks indicate residues identical to those of M-45. The remaining C-terminal 451 residues are identical among the five isolates (see Methods).

Fig. 7. NS3 enhances SEAP secretion from the cells in a sequence-dependent manner. (A) Myc-tagged full-length NS3 of different sequences were coexpressed with SEAP (pSEAP2-Control) and *Renilla* luciferase (pRL-SV40) in HeLa cells, either in the absence (open columns) or presence of

ectopic, full-length ELKS-δ (filled columns). An irrelevant protein (GST) served as a control for NS3. SEAP activities in the medium were measured and normalized to *Renilla* luciferase activities. Percent increase in NS3-mediated SEAP secretion over the control is shown. Mean ± S.D. from three independent experiments. *, $P<0.001$; †, $P<0.01$, compared to the control; ‡, $P<0.05$, compared to the value in the absence of ectopic ELKS-δ expression (open column). (B) Correlation between NS3-mediated enhancement of SEAP secretion (percent increase) and the degree of interaction with ELKS-δ. Correlation coefficient (r) = 0.97973485 ($P<0.0001$). (C) Parental Huh-7, HCV RNA replicon-harbouring Huh-7 and HCV RNA-negative cured Huh-7 cells were cotransfected with pSEAP2-Control and pRL-SV40. SEAP activities in the medium were measured and normalized to *Renilla* luciferase activities. Mean ± S.D. of the relative SEAP secretion compared to the parental Huh-7 is shown. *, $P<0.05$, compared to the parental and cured Huh-7 cells.

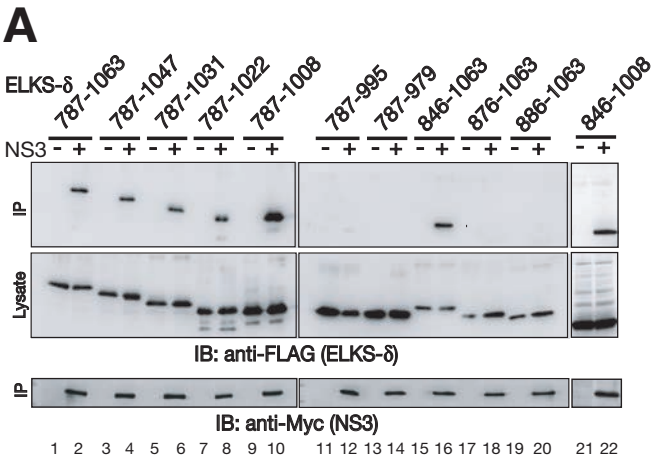


B



	Growth on His(–)	β–Gal activity
1. pLex-NS3-H-31 + pB42-vector	–	–
2. pLex-NS3-H-31 + pB42-ELKS-δ(787-1063)	+	++
3. pLex-NS3-H-31 + pB42-ELKS-δ(787-1063)-FS	–	–
4. pLex-NS3-H-31 + pB42-ATF6-α	–	–
5. pLex-NS3-H-31 + pB42-Jun	–	–
6. pLex-NS3-H-45 + pB42-vector	–	–
7. pLex-NS3-H-45 + pB42-ELKS-δ(787-1063)	+	++
8. pLex-NS3-H-45 + pB42-ELKS-δ(787-1063-FS	–	–
9. pLex-NS3-H-45 + pB42-ATF6-α	–	–
10. pLex-NS3-H-45 + pB42-Jun	–	–
11. pLex-vector + pB42-ELKS-δ(787-1063)	–	–
12. pLex-NS3-H-31-FS + pB42-ELKS-δ(787-1063)	–	–

Fig. 1, Hidajat *et al*.



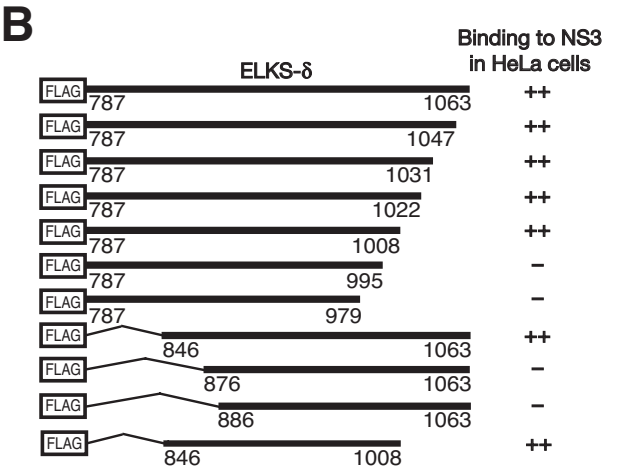


Fig. 2, Hidajat *et al*.

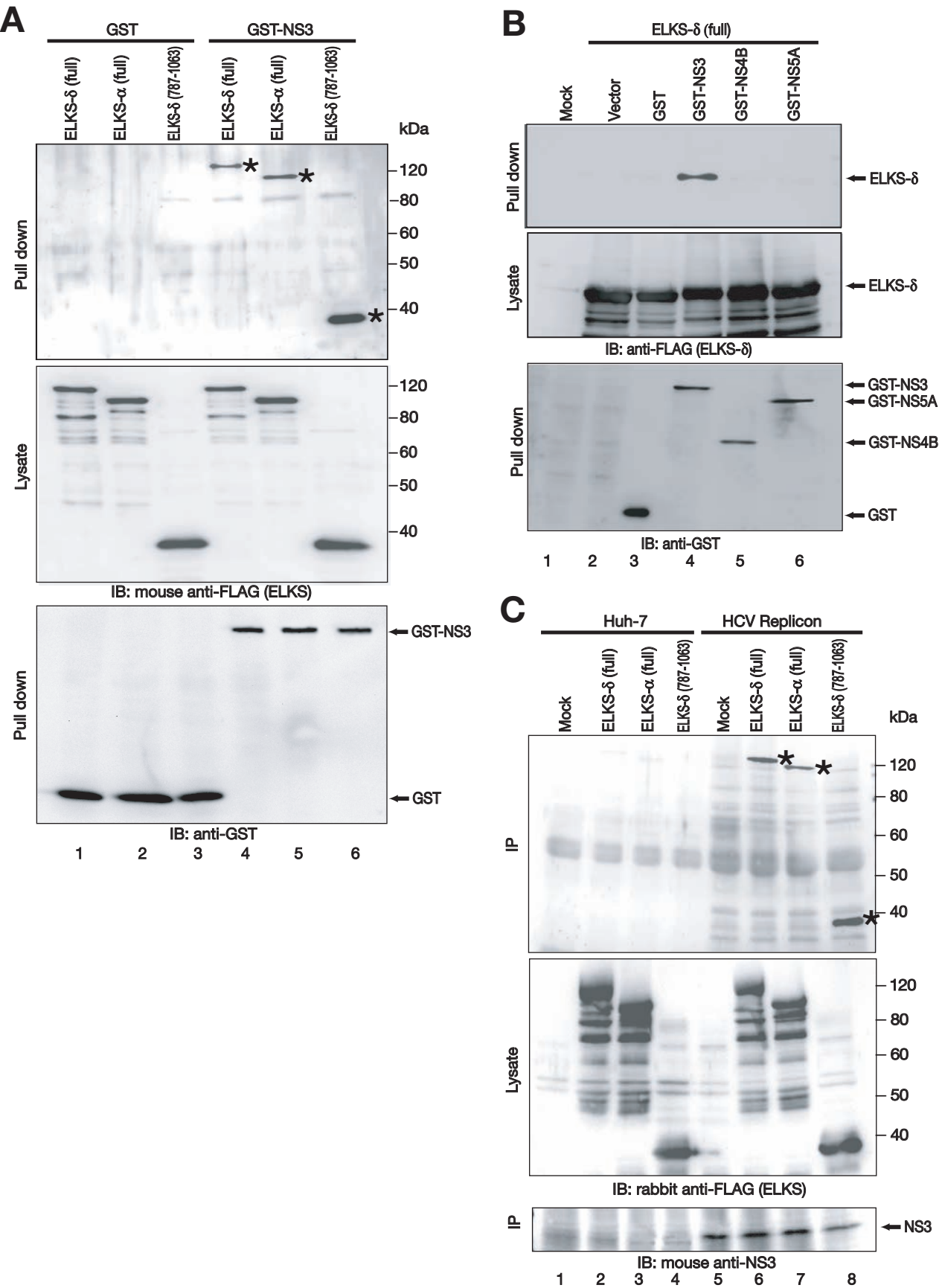


Fig. 3, Hidajat *et al*.

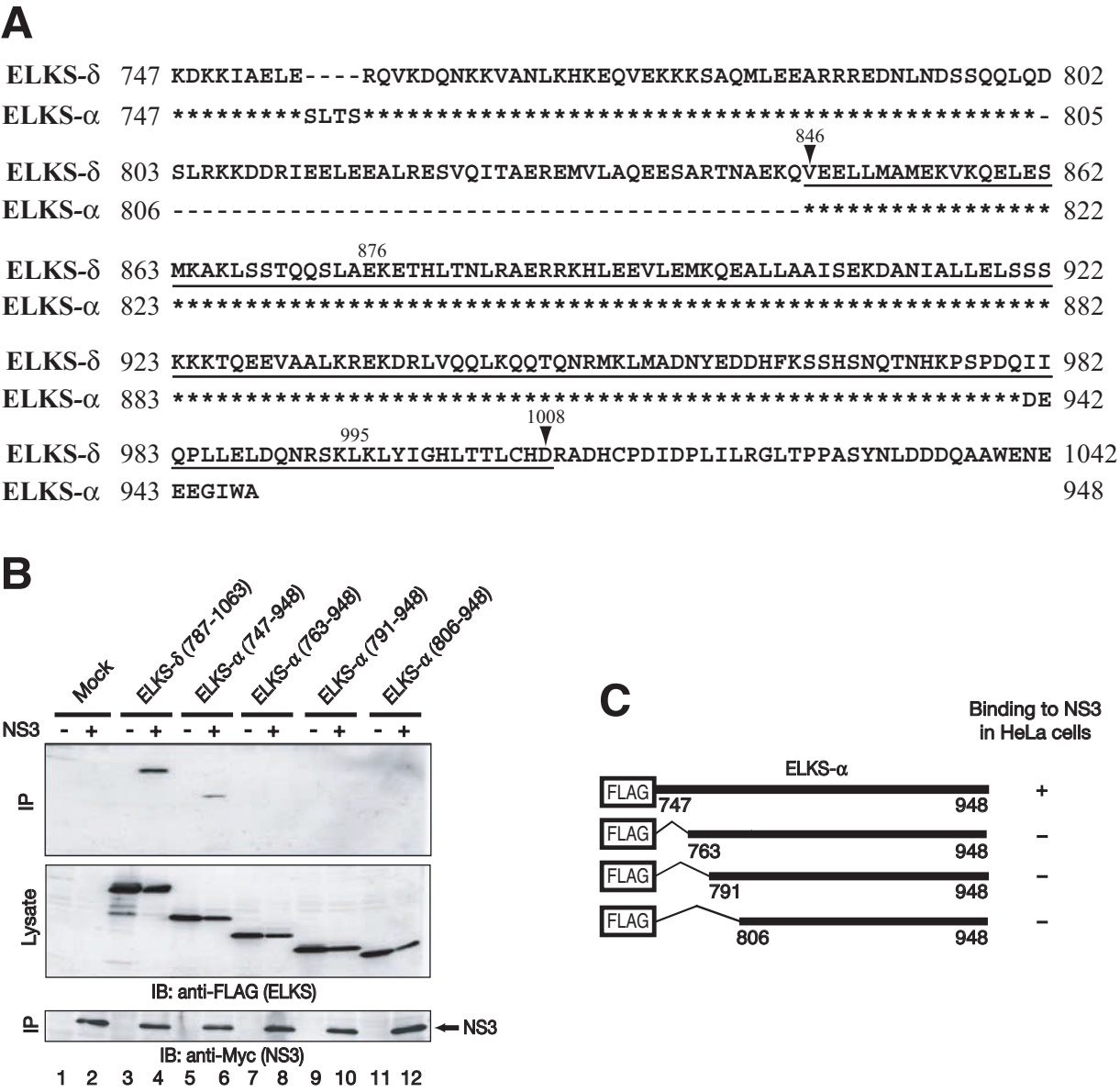


Fig. 4, Hidajat *et al*.

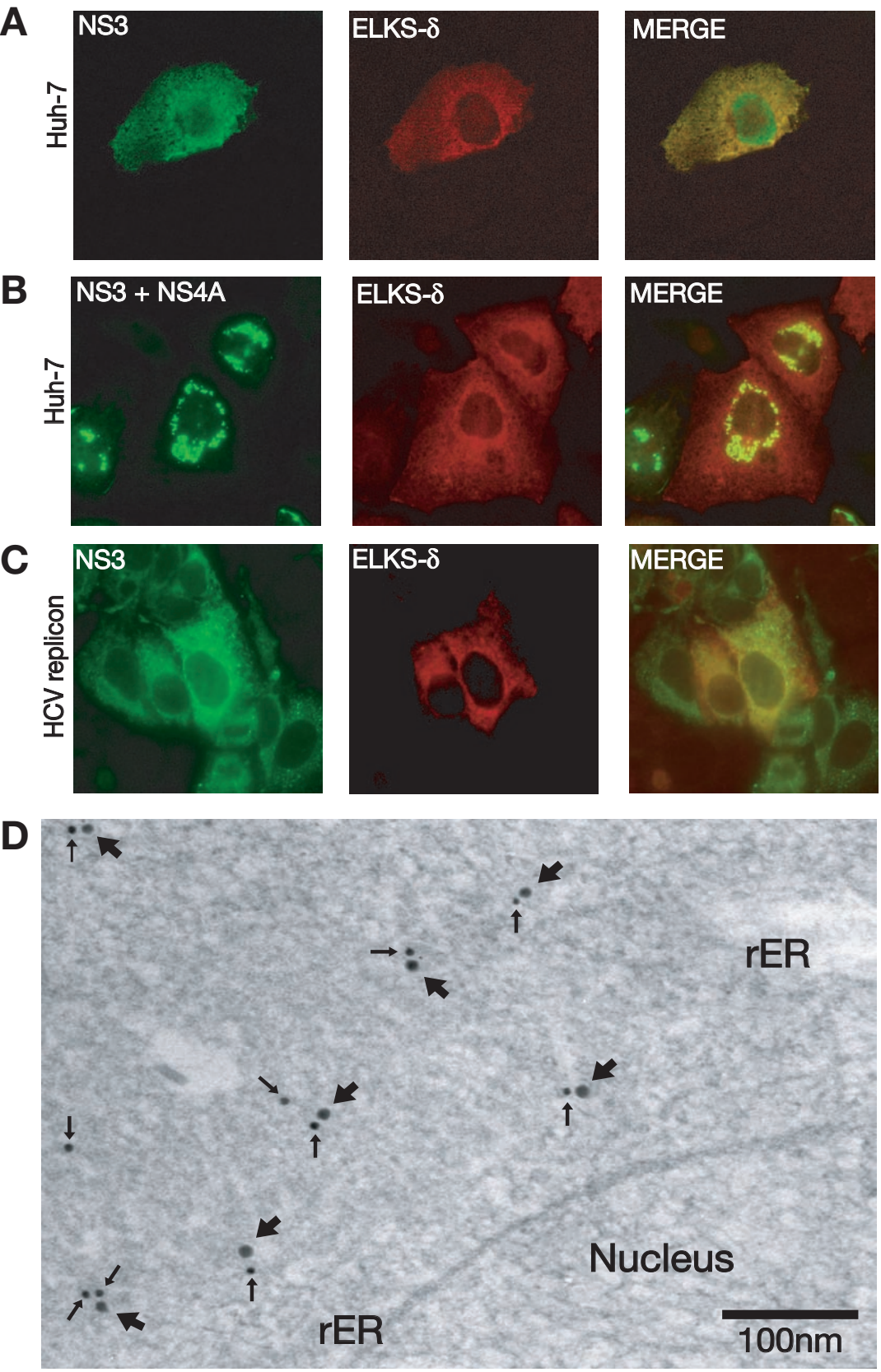
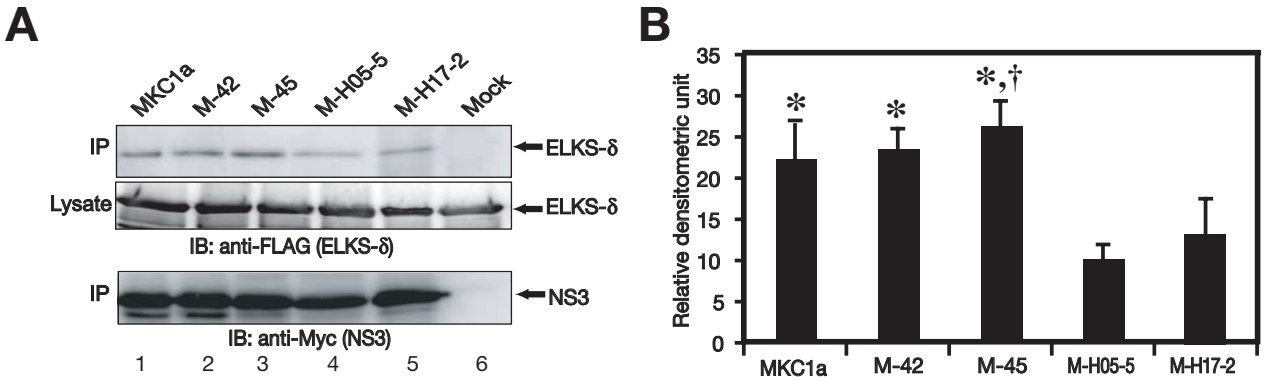


Fig. 5, Hidajat *et al*.



C

```
M-45     1027 APITAYSQQTRGLLGCVITSLTGRDKNQVEGEVQVVSTATQSFLATCVNGVCWTVFHGAG 1086
M-42          ****************I*************************************Y****
MKC1a         ****************I*********************************I*******Y****
M-H17-2       ****************I*************************************Y****
M-H05-5       ****************IV********************************I*******Y****
Replicon      ****************I********R*******************************Y****

M-45     1087 SKTLAGPKGPITQMYTNVDQDLVGWQAPPGARSMTPCTCGSSDLYLVTRHADVIPVRRRG 1146
M-42          **********V**************P*******L**************************
MKC1a         *************************P**********************************
M-H17-2       *******************************S**L**************************
M-H05-5       ******************L*****************************************
Replicon      *********************************L**************************

M-45     1147 DGRGSLLSPRPVSYLKGSSGGPLLCPSGHVVGIFRAAVCTRGVAKAVDFVPVESMETTMR 1206
M-42          *N*************************************************************
MKC1a         *S*********I*************************************************
M-H17-2       *S*********I*************************************************
M-H05-5       *S*************************A**V****************I**********
Replicon      *S*************************A*********************************
```

Fig. 6, Hidajat *et al*.

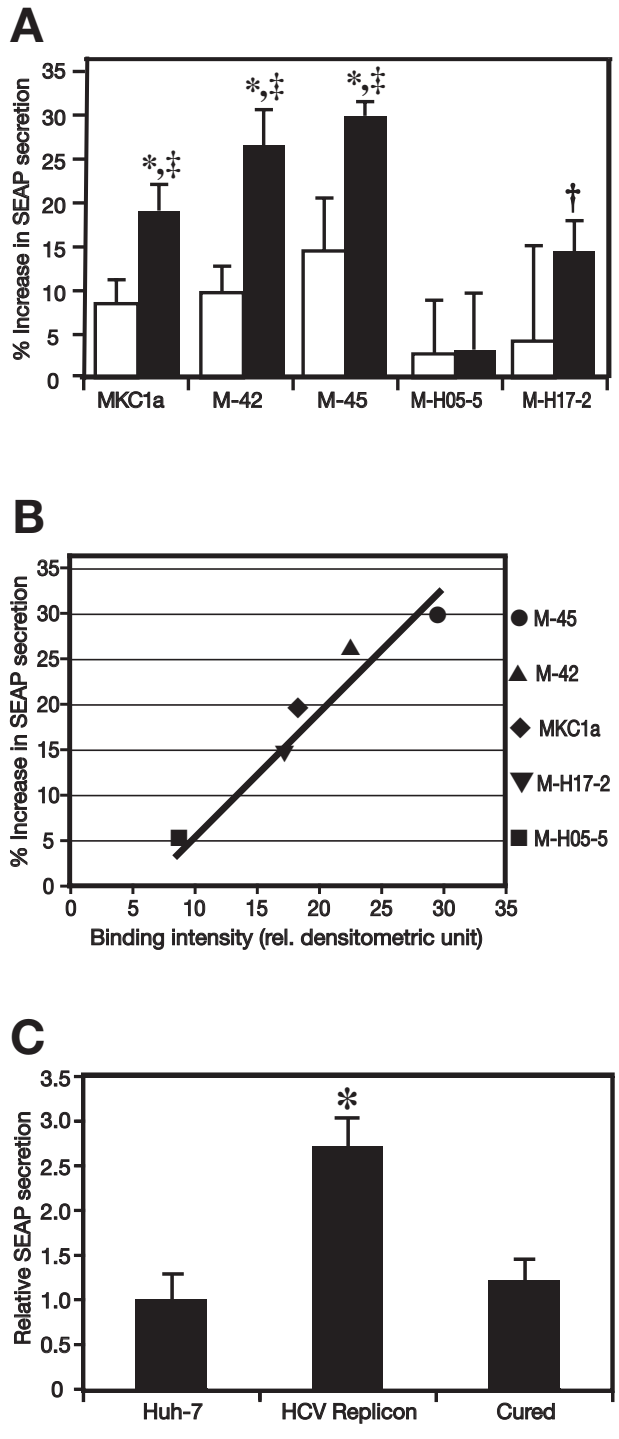


Fig. 7, Hidajat *et al*.